The Common Self-polar Triangle of Concentric Circles and Its Application to Camera Calibration

Haifei Huang[1,2], Hui Zhang[2,3], and Yiu-ming Cheung[1,2]

[1]Department of Computer Science, Hong Kong Baptist University, Hong Kong SAR, China
[2]United International College, BNU-HKBU, Zhuhai, China
[3]Shenzhen Key Lab of Intelligent Media and Speech, Shenzhen, China
{*mikehuang,amyzhang*}*@uic.edu.hk ymc@comp.hkbu.edu.hk*

Abstract

In projective geometry, the common self-polar triangle has often been used to discuss the position relationship of two planar conics. However, there are few researches on the properties of the common self-polar triangle, especially when the two planar conics are special conics. In this paper, we explore the properties of the common self-polar triangle, when the two conics happen to be concentric circles. We show there exist infinite many common self-polar triangles of two concentric circles, and provide a method to locate the vertices of these triangles. By investigating all these triangles, we find that they encode two important properties. The first one is all triangles share one common vertex, and the opposite side of the common vertex lies on the same line, which are the circle center and the line at the infinity of the support plane. The second is all triangles are right triangles. Based on these two properties, the imaged circle center and the varnishing line of support plane can be recovered simultaneously, and many conjugate pairs on vanishing line can be obtained. These allow to induce good constraints on the image of absolute conic. We evaluate two calibration algorithms, whereby accurate results are achieved.

The main contribution of this paper is that we initiate a new perspective to look into circle-based camera calibration problem. We believe that other calibration methods using different circle patterns can benefit from this perspective, especially for the patterns which involve more than two circles.

1. Introduction

In computer vision, camera calibration plays an important role in many applications, such as 3D model recon-struction [13, 12], robot navigation [3] and image-based rendering [11]. The issue of camera calibration includes the estimation of internal parameters, external parameters and lens distortion [22, 28]. Many calibration methods have been presented in past decades [19, 28, 29, 5, 8, 14]. Traditional object-based calibration involves highly accurate tailor-made 3D objects, which usually consist of two or three orthogonal planes [19]. These calibration methods can achieve a high calibration accuracy, but they require an expensive calibration apparatus, and an elaborate setup [28]. Recently, sphere, a common simple 3D object, has been used in calibration [18, 1, 25, 27]. The images of spheres provide good projective constrains on camera calibration, but the size of the sphere, as well as the distance between the sphere and the image center, largely affect the calibration results [22]. To obtain a certain of flexibility and acceptable accuracy, 2D planar pattern has been employed in camera calibration. Roughly, there are two popular types of 2D planar pattern. The first utilizes grid pattern. For instance, Zhang [28] used a planar grid pattern and achieved accurate results. The second one utilizes circular patterns. In [15] , Meng et al. proposed a method using a pattern that consists of a circle and straight lines passing through its centers. Ying and Zha [24] presented a method for camera calibration by using one circle image and one coplanar vanishing point. In [4], Chen et al. provided a novel camera calibration method to estimate the extrinsic parameters and the focal length of a camera by using only one single image of two coplanar circles with arbitrary radius. Further, papers [10, 20, 26] have discussed about the use of concentric circles pattern.

In this paper, we focus on the concentric circles pattern. Previous works always recover the imaged circle center and the vanishing line of the support plane in separate steps. In [10], they put rank-1 constraint on the linear combination

of two concentric circle images to recover the imaged circle center, and put rank-2 constraint to recover the imaged circular points. In [20], they utilized the characteristics of concentric circles tangent lines to locate the center of these circles. In [26], they recovered the imaged circular center by exploring the eigenvalue features of the linear combinations of concentric circles. Note that in [20] and [26], they recovered the imaged circle center, followed by recovering the vanishing line by using pole-polar relationship. In this paper, we recover the imaged circle center and the vanishing line of the support plane simultaneously by investigating the common self-polar triangle [7, 23, 6, 17] of concentric circles. In the literature, the common self-polar triangle has been used to discuss the position relationship between two planar conics [21] and interpret the invariants of two coplanar conics [16]. So far, there are few studies on the properties of the common self-polar triangles of coplanar conics, especially when the two conics are special conics. Accordingly, we explore the properties of the common self-polar triangle, when the two conics happen to be concentric circles. We show there exist infinite many common self-polar triangles of two concentric circles, and provide a method to locate the vertices of these triangles. By investigating all these triangles, we find that they encode two important properties. The first one is all triangles share one common vertex, and the opposite side of the common vertex lies on the same line, which are the circle center and the line at the infinity of the support plane. The second is all triangles are right triangles. Based on these two properties, the imaged circle center and the varnishing line of support plane can be recovered simultaneously, and many conjugate pairs on vanishing line can be obtained from the image of two concentric circles. These allow to induce good constraints on the image of absolute conic (IAC). In the application, we evaluate two calibration algorithms, whereby accurate results are achieved. The main contribution of this paper is that we initiate a new perspective to look into circle based camera calibration problem. It is expected that other calibration methods using different circle patterns can benefit from this perspective, especially for the patterns which involve more than two circles.

The remainder of this paper is organized as follows. Section 2 briefly introduces some notations and basic equations. Section 3 discusses the properties of common self-polar triangle of two concentric circles. Section 4 presents our novel method to recover the imaged circle center and vanishing line, and describes calibration methods. Section 5 shows the experimental results on synthetic and real data sets. Finally, the concluding remarks are drawn in Section 6.
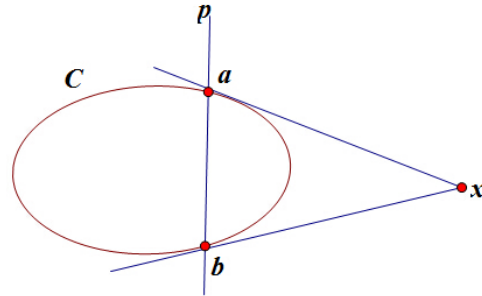

Figure 1. The pole-polar relationship, where line p is the polar of the point $\mathbf{x}$ with respect to conic $\mathbf{C}$.

2. Preliminaries

2.1. Camera Model

The pinhole camera model is adopted in this paper. In the homogenous coordinate system, let $\mathbf{m}=[x\ y\ x\ 1]^{\mathbf{T}}$ be a world point and $\widetilde{\mathbf{m}}=[x\ y\ 1]^{\mathbf{T}}$ be its image. The imaging process can be represented as

$$u\widetilde{\mathbf{m}}=\mathbf{K}[\mathbf{R}|\mathbf{t}]\mathbf{m}, \tag{1}$$

where u is a nonzero scale factor, $\mathbf{R}|\mathbf{t}$ denotes a rigid transformation, and $\mathbf{K}$ is the intrinsic parameter matrix with the following format:

$$\mathbf{K}=\begin{bmatrix} \alpha f & s & u_0 \\ 0 & f & v_0 \\ 0 & 0 & 1 \end{bmatrix}. \tag{2}$$

In the matrix $\mathbf{K}$, f is the focal length, α is the aspect ratio, (u_0, v_0) is the principal point, and s is the skew.

2.2. The Absolute Conic

The absolute conic is a point conic on infinite plane. Point $\mathbf{x}=[x_1\ x_2\ x_3\ x_4]$ on absolute conic satisfy

$$x_1^2 + x_2^2 + x_3^2 = 0, x_4 = 0. \tag{3}$$

The image of the absolute conic ω is the conic $\mathbf{K}^{-\mathbf{T}}\mathbf{K}^{-1}$ and its dual ω^* (DIAC) is $\mathbf{K}\mathbf{K}^{\mathbf{T}}$ [9]. If enough constraints could be inferred from images, the intrinsic parameters $\mathbf{K}$ can be determined by Cholesky decomposition [7].

2.3. Pole-polar Relationship and Self-polar Triangle

A point $\mathbf{x}$ and conic $\mathbf{C}$ define a line $p = \mathbf{C}\mathbf{x}$. The line p is called the polar of $\mathbf{x}$ with respect to $\mathbf{C}$, and the point $\mathbf{x}$ is the pole of p with respect to $\mathbf{C}$ (see Figure 1).

If the poles of a conic form the vertices of a triangle and their respective polars form its opposite sides, it is called

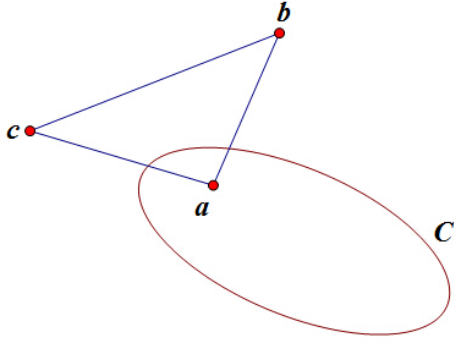Figure 2. $\triangle \mathbf{abc}$ is a self-polar triangle with respect to conic $\mathbf{C}$ when polars of a, b and c are lines bc, ac and ab, respectively.
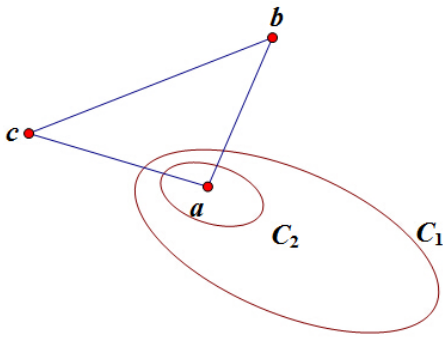

Figure 3. $\triangle \mathbf{abc}$ is the common self-polar triangle of two disjoint conics $\mathbf{C}_1$ and $\mathbf{C}_2$ when $\triangle \mathbf{abc}$ is a self-polar triangle with respect to both $\mathbf{C}_1$ and $\mathbf{C}_2$.

a self-polar triangle (see Figure 2). If a self-polar triangle is common to two conics, it is called common self-polar triangle (see Figure 3) [23].

For the sake of discussion in the coming sections, we recall two theorems related to pole-polar as follows.

Theorem 1. The polar line $p = \mathbf{Cx}$ of the point $\mathbf{x}$ with respect to a conic $\mathbf{C}$ intersects the conic in two points. The two lines tangent to $\mathbf{C}$ at these points intersect at $\mathbf{x}$.

Theorem 2. If $\mathbf{x}$ is on the polar of $\mathbf{y}$ then $\mathbf{y}$ is on the polar of $\mathbf{x}$.

Proof and more details about these two theorems could be found in [9].

3. Properties of Common Self-polar Triangle of Concentric Circles

In this section, we prove one proposition first. From this proposition, we then obtain two properties of the common self-polar triangle of concentric circles.

Proposition 1. Two concentric circles have infinite many common self-polar triangles.

Proof. Let $\mathbf{o}$ be the circle center of $\mathbf{C}_1$ and $\mathbf{C}_2$ and l be the line at infinity of the support plane. The circle center and the line at infinity are in pole-polar relationship [9]. We have

$$\begin{aligned} l &= \lambda_1 \mathbf{C}_1 \mathbf{o} \\ l &= \lambda_2 \mathbf{C}_2 \mathbf{o}, \end{aligned} \tag{4}$$

where λ_1 and λ_2 are scalar parameters. Obviously, $\mathbf{o}$ and l are a common pole and polar of $\mathbf{C}_1$ and $\mathbf{C}_2$.

Consider a point $\mathbf{y}$ on l. The polar of $\mathbf{y}$ with respect to $\mathbf{C}_1$ and $\mathbf{C}_2$ are:

$$\begin{aligned} p_1 &= \beta_1 \mathbf{C}_1 \mathbf{y} \\ p_2 &= \beta_2 \mathbf{C}_2 \mathbf{y}, \end{aligned} \tag{5}$$

where β_1 and β_2 are scalar parameters.

According to Theorem 2, the circle center is at lines p_1 and p_2.

Let p_1 intersect $\mathbf{C}_1$ in point $\mathbf{a}$ and point $\mathbf{b}$, and p_2 intersect $\mathbf{C}_2$ in point $\mathbf{c}$ and $\mathbf{d}$. From Theorem 1, we get that $\mathbf{ay}$ is the tangent line of $\mathbf{C}_1$, and $\mathbf{cy}$ is the tangent line of $\mathbf{C}_2$. Since $\mathbf{o}$ is the concentric center of $\mathbf{C}_1$ and $\mathbf{C}_2$, we have

$$\begin{aligned} \mathbf{oa} &\perp \mathbf{ay} \\ \mathbf{oc} &\perp \mathbf{cy}. \end{aligned} \tag{6}$$

Note that $\mathbf{ay}$ and $\mathbf{cy}$ intersect at infinity, which means in Euclidean space, the line $\mathbf{ay}$ and $\mathbf{cy}$ are parallel. Consequently, we know that p_1 and p_2 are parallel. Since they share one common point $\mathbf{o}$, p_1 and p_2 are the same line.

Let p_1 intersect infinity line l in point $\mathbf{z}$. Since point $\mathbf{z}$ is on l, the polar of z goes through $\mathbf{o}$. Besides, point $\mathbf{z}$ is on line p_1, the polar of $\mathbf{z}$ goes through $\mathbf{y}$. Based on those, the polar of $\mathbf{z}$ with respect to $\mathbf{C}_1$ and $\mathbf{C}_2$ is $\mathbf{oy}$, which means $\triangle \mathbf{zoy}$ is a self-polar triangle. Since $\mathbf{y}$ is randomly chosen, it implies that there are infinite many self-polar triangle of concentric circles. $\square$

From the details of the proof, we observe two properties of the common self-polar triangles of two concentric circles.

Property 1. All common self-polar triangles of two concentric circles share one common vertex and the opposite side of this vertex lies on the same line, which are the circle center and the line at infinity of the support plane.

Property 2. All common self polar triangles of two concentric circles are right triangles.

We give some interpretations on Property 2. In the process of proof for Proposition 1, we know that ya and yo intersect in point y at infinity, which means lines ya and yo are parallel. Besides, oa is orthogonal to ya. Consequently, oa is orthogonal to yo. Thus, $\triangle \mathbf{zoy}$ is a right triangle.
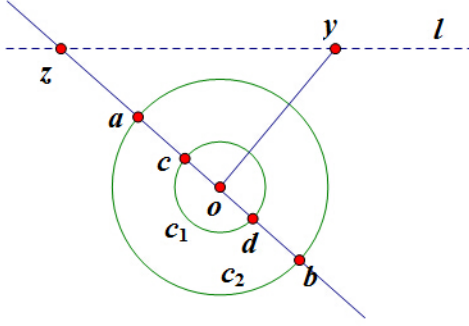
Figure 4. C_1 and C_2 are two concentric circles, where circle center is o, l is the line at infinity of the support plane, and $\triangle zoy$ is a self-polar triangle with $zo \perp yo$.

3.1. The Common Vertex and the Opposite Line Recovery

From Property 1, we obtain that the common vertex of the common self-polar triangles is the circle center and the opposite line is the line at infinity. In this section, we show the process to recover the common vertex and the opposite line.

Without loss of generality, let the circles center be $[x_0 \ y_0 \ 1]^{\mathbf{T}}$ (homogenous representation) and radii be r_1 and r_2. The matrix representations of C_1 and C_2 are

$$C_1 = \begin{bmatrix} 1 & 0 & -x_0 \\ 0 & 1 & -y_0 \\ -x_0 & -y_0 & x_0^2 + y_0^2 - r_1^2 \end{bmatrix} \quad (7)$$

and

$$C_2 = \begin{bmatrix} 1 & 0 & -x_0 \\ 0 & 1 & -y_0 \\ -x_0 & -y_0 & x_0^2 + y_0^2 - r_2^2 \end{bmatrix}. \quad (8)$$

From Proposition 1, we know that C_1 and C_2 have infinite common self-polar triangles, which indicate they have infinite common pole-polars. Let point $\mathbf{x}$ and line p be the common pole-polar of C_1 and C_2. The following relationship should be satisfied:

$$\begin{aligned} p &= C_1 \mathbf{x} \\ p &= \lambda C_2 \mathbf{x}, \end{aligned} \quad (9)$$

where λ is a scalar parameter. Subtracting the equations in (9), we get $(C_1 - \lambda C_2)x = 0$. By multiplying the inverse of C_2 on both sides, we obtain the following equation:

$$(C_2^{-1} C_1 - \lambda \mathbf{I}) \mathbf{x} = 0. \quad (10)$$

From equation (10), we find the common poles for C_1 and C_2 are the eigenvectors of $C_2^{-1} C_1$. We use the matlab

code $[\mathbf{V}, \mathbf{D}] = \mathbf{eig}(\mathbf{C2}, \mathbf{C1})$ to calculate the eigenvectors and eigenvalues. We obtain

$$\mathbf{V} = \begin{bmatrix} 1 & 0 & x_0 \\ 0 & 1 & y_0 \\ 0 & 0 & 1 \end{bmatrix} \quad (11)$$

and

$$\mathbf{D} = \begin{bmatrix} 1 & 0 & 0 \\ 0 & 1 & 0 \\ 0 & 0 & r_1^2/r_2^2 \end{bmatrix}. \quad (12)$$

From matrix D, we find that $C_2^{-1} C_1$ has three eigenvalues, of which two are identical and one is different. From matrix V, we find that the corresponding eigenvectors of the identical eigenvalues are $[1 \ 0 \ 0]^{\mathbf{T}}, [0 \ 1 \ 0]^{\mathbf{T}}$, which are points on infinity line. We also find the corresponding eigenvector of the different eigenvalue is $[x_0 \ y_0 \ 1]^{\mathbf{T}}$, which is the circle center. Based on the above analysis, we can conclude that the circle center and the line at infinity can be recovered by the eigenvector s of the matrix $C_2^{-1} C_1$.

4. Calibration Theory

4.1. The Images of Two Concentric Circles

Let the images of two concentric circles under projection matrix $\mathbf{H}$ be $\widetilde{C_1}$ and $\widetilde{C_2}$. We have:

$$\begin{aligned} \widetilde{C_1} &= \mathbf{H}^{-\mathbf{T}} C_1 \mathbf{H}^{-1} \\ \widetilde{C_2} &= \mathbf{H}^{-\mathbf{T}} C_2 \mathbf{H}^{-1}. \end{aligned} \quad (13)$$

By computing the product $\widetilde{C_2}^{-1} \widetilde{C_1}$, we obtain:

$$\begin{aligned} \widetilde{C_2}^{-1} \widetilde{C_1} &= (\mathbf{H}^{-\mathbf{T}} C_2 \mathbf{H}^{-1})^{-1} (\mathbf{H}^{-\mathbf{T}} C_1 \mathbf{H}^{-1}) \\ &= \mathbf{H}(C_2^{-1} C_1) \mathbf{H}^{-1}. \end{aligned} \quad (14)$$

We find that $\widetilde{C_2}^{-1} \widetilde{C_1}$ is similar to $C_2^{-1} C_1$. If λ and $\mathbf{x}$ are eigenpair of $C_2^{-1} C_1$, according to the property of similarity transformation, λ and $\mathbf{Hx}$ are eigenpair of $\widetilde{C_2}^{-1} \widetilde{C_1}$. Considering the facts in Subsection 3.1, we know that the imaged circle center and vanishing line can be recovered by the eigenvectors of the matrix $\widetilde{C_2}^{-1} \widetilde{C_1}$. Subsequently, the recovery algorithm is given as follows:

Step 1: Extract two concentric circles images $\widetilde{C_1}$ and $\widetilde{C_2}$.
Step 2: Compute $(\lambda, \mathbf{x})$ of $\widetilde{C_1}$ and $\widetilde{C_2}$. Let three eigenpairs be $(\lambda_1, \mathbf{x_1})$, $(\lambda_2, \mathbf{x_2})$, and $(\lambda_3, \mathbf{x_3})$, in which the values of λ_2 and λ_3 are identical.
Step 3: Calculate the cross product of $\mathbf{x_2}$ and $\mathbf{x_3}$ and let it be v. The imaged circle center is $\mathbf{x_1}$ and the vanishing line is v.

4.2. Calibration Methods

Based on the properties of the common self-polar triangle of concentric-circles, we present two calibration algorithms.

4.2.1 Calibration Method Based on the Common Line of the Common Self-polar Triangles

From Section 4.1, we know how to recover the vanishing line. Once the vanishing line is recovered, imaged circular points can be obtained by intersecting the circle image with the vanishing line. One pair of imaged circular points provides two independent constraints on IAC. Given at least three views of two concentric circles, we can fully calibrate the camera [9]. The complete calibration algorithm consists of the following steps:

Step 1: Extract the images of two concentric circles $\widetilde{\mathbf{C}}_1$ and $\widetilde{\mathbf{C}}_2$.

Step 2: Calculate the eigenvectors of $\widetilde{\mathbf{C}}_2^{-1}\widetilde{\mathbf{C}}_1$. Then, recover the vanishing line.

Step 3: Find the imaged circular points by intersecting the circle image with the vanishing line.

Step 4: For three views, repeat the above steps three times.

Step 5: Determine IAC by using imaged circular points and obtain K using the Cholesky factorization.

4.2.2 Calibration Method Based on Orthogonality of the Common Self-Polar Triangles

From Proposition 1, we observe that all common self-polar triangles are right triangle. One orthogonality provides one constraint on IAC [9]. If we try to calibrate the camera, we need to consider more common self-polar triangle in one image. Note that only two of them are independent. Therefore, at least three views should be provided. The complete calibration algorithm consists of the following steps:

Step 1: Extract the images of two concentric circles $\widetilde{\mathbf{C}}_1$ and $\widetilde{\mathbf{C}}_2$.

Step 2: Calculate the eigenvectors of $\widetilde{\mathbf{C}}_2^{-1}\widetilde{\mathbf{C}}_1$. Then, recover the imaged circle center ant the vanishing line.

Step 3: Randomly form two common self-polar triangles and calculate the conjugate pairs.

Step 4: For three views, repeat the above steps three times.

Step 5: Determine IAC by using orthogonality and obtain K using the Cholesky factorization.

5. Experiments and Results

5.1. Synthetic Data

In the computer simulations, the simulated camera setup is the same as the one in [28]: $f = 900$, aspect ratio $\alpha f = 1250$, skew $s = 1.09083$, and principal point $(u_0, v_0) = (255, 255)$. The image resolution is: 512×512. The model pattern is circles pattern containing two concentric circles. In this experiment, we move the camera to obtain three images of the pattern. We choose 20 points on each circle image. Gaussian noise with zero-mean and σ standard deviation is added to these image points. Ellipses are fitted to
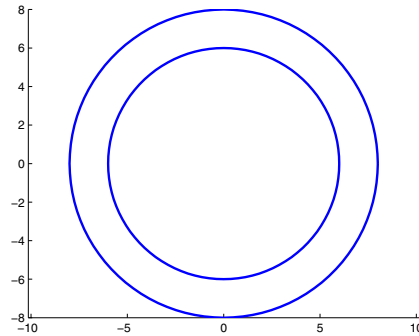

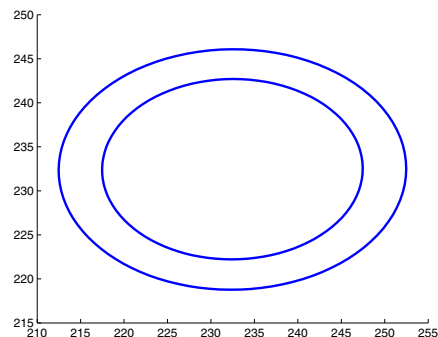Figure 5. Two concentric circles generated by computer.

Figure 6. One image produced by simulated camera.

Approach	αf	f	u_0	v_0
Ground-truth	1250	900	255	255
Our method(0.2)	1237.2	896.5	258.3	252.1
Our method(0.4)	1252.4.9	894.4	270.1	304.1

Table 1. Camera calibration results with the noise level at 0.2 pixel and 0.4 pixel, respectively.

these images using a least squares ellipse fitting algorithm. We vary the noise level form 0.1 pixel to 0.5 pixel. For each noise level, we conduct 15 independent trials, and the final averaged results are shown. Since the above two calibration algorithms both largely depend on the vanishing line recovery, the calibration results have a small difference. As we can see from Fig.6 and Fig.7, errors increase linearly over the noise level. In Table 1, we show the calibration results with the noise level at 0.2 pixel and 0.4 pixel, respectively.

We generalize our results to two sets of concentric circles and three concentric circles. For this experiment, we choose 100 points to fit the ellipse and conduct 15 independent trials for each noise level. As we can see from Fig.11, the other two patterns are better than two concentric circles. In Table 2, we show the calibration results with the noise
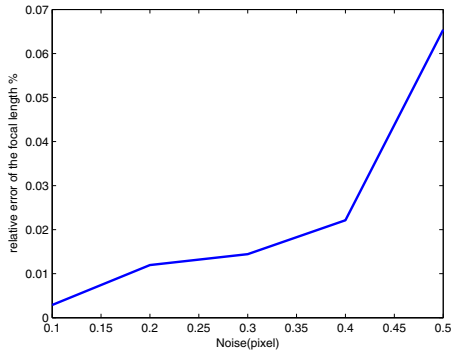
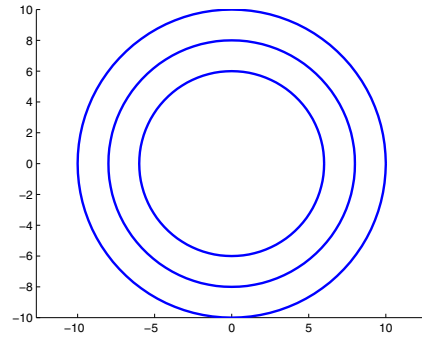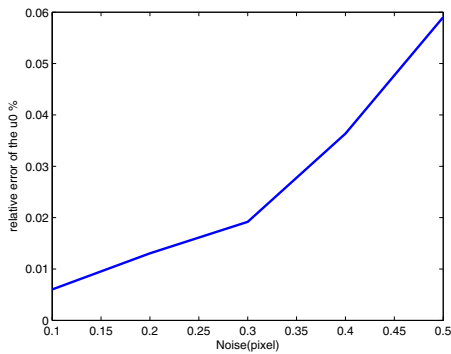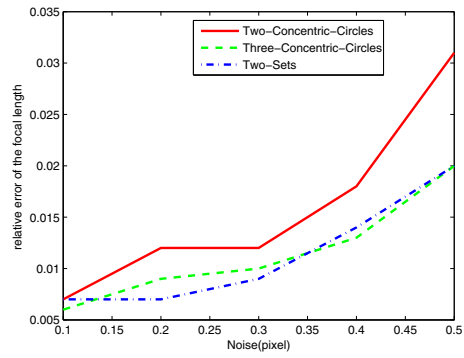Figure 7. The relative focal length errors vs. the noise level of the image points.

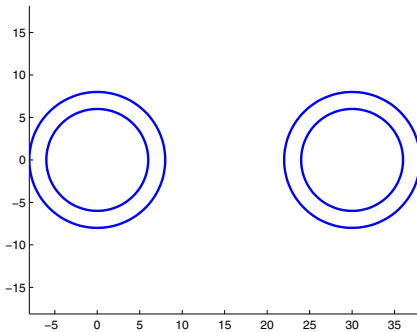Figure 8. The relative u_0 errors vs. the noise level of the image points.

Figure 9. Two sets of concentric circles synthesized by computer.

level at 0.2 pixel and 0.4 pixel, respectively, for the three different patterns.

5.2. Real Scene

In the real scene experiment, real images are taken with a Nikon D300s camera. The image resolution is 2144×1244.

Figure 10. Three concentric circles synthesized by computer.

Figure 11. The relative focal length errors vs. the noise level of the image points.

Approach	αf	f	u_0	v_0
Ground-truth	1250	900	255	255
Two circles(0.2)	1233.2	889.4.5	254.3	247.9
Two sets(0.2)	1235.2	893.5	256.3	245.7
Three circles(0.2)	1238	892.2	256.7	250.5
Two circles(0.4)	1219.6	883.9	260	255
Two sets(0.4)	1223.3	887.7	256.3	246.3
Three circles(0.4)	1223.1	888.2	263.1	250.1

Table 2. Camera calibration results with the noise level at 0.2 pixel and 0.4 pixel, respectively.

The images of circles are extracted using Canny edge detector [2], and ellipses are fitted to these images using a least squares ellipse fitting algorithm. The camera is calibrated with the proposed approach. The estimated parameters are listed in Table 3, where the result from the method of Kim [10] is taken as the ground truth. From the results, we find that both methods have small difference. It is believed that the difference is caused by accumulated errors due to different steps involved in the methods.
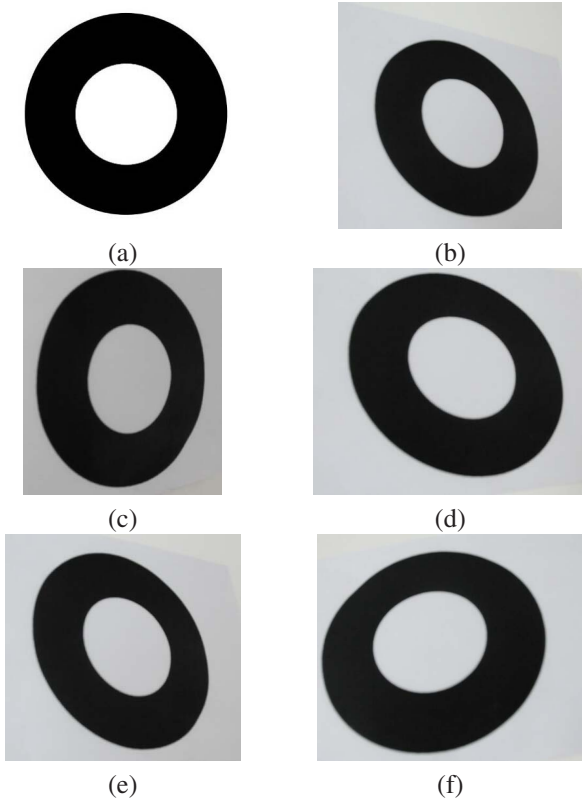
Figure 12. (a) The real two concentric circles. (b-e) Five views of two concentric circles.

Approach	αf	f	s	u_0	v_0
Kim method	1705.3	1625.6	6.4	1088	541
Our method	1705.4	1628.3	7.5	1082.6	537.6

Table 3. Real experiment results: 5 views.

6. Concluding Remarks

We have investigated the properties of the common self-polar triangles of two concentric circles. We have shown that the properties can be well used in camera calibration and the promising results have been achieved. It is believed that the self-polar triangle can be used in other circle patterns. Based on our studies, we find each of two disjoint circles has a unique self-polar triangle, one vertex of which lies on the line at infinity. Given more than two disjoint circles, more than two self-polar triangles can be recovered, the vertex of which can be used to recover the vanishing line. By using this method, we can avoid solving quartic equation, which may cause numerical instability [10]. In the future, we will focus on developing a unified calibration method for planar patterns, which include more than two disjoint circles.

References

[1] M. Agrawal and L. S. Davis. Camera calibration using spheres: A semi-definite programming approach. In *Proc. of IEEE International Conf. on Computer Vision*, pages 782–789, 2003.

[2] J. Canny. A computational approach to edge detection. *IEEE Trans. on Pattern Analysis and Machine Intelligence*, 8(6):679–698, 1986.

[3] H. Chen, K. Matsumotob, J. Otac, and T. Araic. Self-calibration of environmental camera for mobile robot navigation. *Robotics and Autonomous Systems*, 55(3):177–190, 2007.

[4] Q. Chen, H. Y. Wu, and T. Wada. Camera calibration with two arbitrary coplanar circles. In *Proc. European Conf. on Computer Vision*, pages 521–532, 2004.

[5] O. D. Faugeras, Q. T. Luong, and S. J. Maybank. Camera self-calibration: Theory and experiments. In *Proc. ECCV*, pages 321–334, 1992.

[6] L. N. G. Filon. *Introduction to Projective Geometry*. Edward Arnold, 1908.

[7] J. E. Gentle. *Numerical Linear Algebra for Applications in Statistics*. Springer-Verlag, 1998.

[8] R. Hartley. An algorithm for self calibration from several views. In *Proc. IEEE Conference on Computer Vision and Pattern Recognition*, pages 2205–2216, 2007.

[9] R. Hartley and A. Zisserman. *Multiple View Geometry in Computer Vision*. Cambridge University, 2000.

[10] J. S. Kim, P. Gurdjos, and I. S. Kweon. Geometric and algebraic constraints of projected concentric circles and their applications to camera calibration. *IEEE Trans. on Pattern Analysis and Machine Intelligence*, 27(4):637–642, 2005.

[11] S. Laveau and O. D. Faugeras. 3-d scene representation as a collection of images. In *Proc. International Conference on Pattern Recognition*, volume A, pages 689–691, 1994.

[12] C. Liang and K. Y. K. Wong. Robust recovery of shapes with unknown topology from the dual space. *IEEE Trans. on Pattern Analysis and Machine Intelligence*, 29(12):2205–2216, 2007.

[13] W. N. Martin and J. K. Aggarwal. Volumetric descriptions of objects from multiple views. *IEEE Trans. on Pattern Analysis and Machine Intelligence*, 5(2):150–158, 1983.

[14] S. J. Maybank and O. D. Faugeras. A theory of self-calibration of a moving camera. *International Journal of Computer Vision*, 8(2):123–151, 1992.

[15] X. Q. Meng, H. Li, and Z. Y. Hu. A new easy camera calibration technique based on circular points. In *Proc. British Mashion Vision Conference*, volume 29, pages 2205–2216, 2007.

[16] L. Quan, P. Gros, and R. Mohr. Invariants of a pair of conics revisited. In *Proceedings of the British Machine Vision Conference*, pages 71–77, 1991.

[17] J. Semple and G. Kneebone. *Algebraic Projective Geometry*. Oxford Science, 1952.

[18] H. Teramoto and G. Xu. Camera calibration by a single image of balls: From conics to the absolute conic. In *Proc. of 5th ACCV*, pages 499–506, 2002.

[19] R. Y. Tsai. A versatile camera calibration technique for high accuracy 3d machine vision metrology using off-the-shelf tv cameras and lenses. *IEEE Journal of Robotics and Automation*, 3(4):323–344, 1987.

[20] L. Wang and H.Yao. Effective and automatic calibration using concentric circles. *International Journal of Pattern Recognition and Artificial Intelligence*, 22(7):1379–1401, 2008.

[21] S. N. R. Wijewickrema, A. P. Paplinski, and C. E. Esson. Tangency of conics and quadrics. In *Proc. of Conf. on Signal Prcossing, Computational Geometry & Artifical Vision*, pages 21–29, 2006.

[22] K. Y. K. Wong, G. Zhang, and Z. Chen. A stratified approach for camera calibration using spheres. *IEEE Trans. on Image Processing*, 20(2):305–316, 2011.

[23] F. S. Woods. *Higher Geometry*. Ginn and Company, 1922.

[24] X. Ying and H.Zha. Camera calibration from a circle and a coplanar point at infinity with application to sports scenes ananlysis. pages 220–225, 2007.

[25] X. Ying and H. Zha. Geometric interpretations of the relation between the image of the absolute conic and sphere images. *IEEE Trans. on Pattern Analysis and Machine Intelligence*, 28(12):2031–2036, 2006.

[26] B. W. Zhang, Y. F. Li, and S. Y. Chen. Concentric-circle-based camera calibration. *IET Image Processing*, 6(7):870–876, 2012.

[27] H. Zhang, G. Zhang, and K. Y. K. Wong. Camera calibration from images of spheres. *IEEE Trans. on Pattern Analysis and Machine Intelligence*, 29(3):499–503, 2007.

[28] Z. Zhang. A flexible new technique for camera calibration. *IEEE Trans. on Pattern Analysis and Machine Intelligence*, 22(11):1330–1334, 2000.

[29] Z. Zhang. Camera calibration with one-dimensional objects. *IEEE Trans. on Pattern Analysis and Machine Intelligence*, 26(7):892–899, 2004.